Structures 51 (2023) 1934–1943

Contents lists available at ScienceDirect

Structures

journal homepage: www.elsevier.com/locate/structures

Application of tuned viscous mass damper isolation systems for equipment-induced vibration control of industrial buildings

Zhengrong Zhu [a,d], Yun Zhou [a,d], Zhongkun Tan [b,c], Hui He [b,*], Xiaofeng Zhou [a,d]

[a] College of Civil Engineering, Hunan University, Changsha 410082, China
[b] Hunan Institute of Technology, Hengyang 421002, China
[c] Hunan Zhongteng Structural Technology Group Co. LTD, Changsha 410012, China
[d] Key Laboratory for Damage Diagnosis of Engineering Structures of Hunan Province, Hunan University, Changsha 410082, China

ARTICLE INFO

Keywords:
Tuned viscous mass damper
Inerter-based devices
TVMD isolation system
Industrial buildings
Closed-form solution

ABSTRACT

Tuned viscous mass dampers (TVMDs) are promising inerter-based devices for vibration control of civil structures. Previous studies chiefly focused on the vibration control performance of TVMDs for a main structure subjected to seismic excitations. In this study, the application of TVMD isolation systems for equipment-induced vibration control of industrial buildings is explored. A closed-form solution for optimum design parameters of TVMD isolation systems is proposed based on the fixed-point theory. The design procedure of TVMD isolation systems is provided to balance the vibrations of the main structure and equipment. The validation of TVMD isolation systems is conducted based on a real industrial building. The numerical analysis results show that TVMD isolation systems optimally designed using the proposed closed-form solution are highly effective in controlling the acceleration and displacement responses of both the main structure and equipment. Moreover, the results confirm that TVMD isolation systems can be used as an effective control strategy to solve the comfort problem of industrial buildings induced by rotary mechanical equipment. This is because the inner degree of freedom in a TVMD is amplified when the TVMD is tuned to resonate with the main structure, which provides a significantly improved energy-dissipation ability of the TVMD isolation system.

1. Introduction

Structural control plays a crucial role in the design and retrofitting of civil structures to avoid damage from undesired vibrations caused by external excitations [1–3]. In particular, a large number of passive control devices have been developed and installed to mitigate undesired vibrations in civil structures [4]. Owing to the significant mass amplification effects of inerter elements, inerter-based devices are widely accepted as effective passive control devices [5]. In recent years, performance testing of inerter-based devices has been conducted in many fields, such as dynamic vibration absorbers in mechanical systems [6,7], buildings [8–15], bridges [16], storage tanks [17–19], wind turbine towers [20], platforms [21], and isolation systems [22]. Isolation systems not only prolong the natural period of the main structure but also dissipate input energy [23]. Hence, the seismic response of isolated structures can be significantly suppressed [24]. However, isolation systems may undergo large displacements under severe seismic excitations [25]. To reduce the displacement and improve the performance of isolation systems, inerter-based isolation systems that combine isolation systems with inerter-based devices provide attractive alternatives to conventional isolation systems [26–28].

The aforementioned inerter element is a two-terminal element that provides an inertial force proportional to the relative acceleration of both terminals [29–34]. In civil engineering, the bud of a two-terminal inerter element is a liquid mass pump developed by Kawamata [35] in the 1970 s. Subsequently, Ikago and his co-workers [36,37] developed a tuned viscous mass damper (TVMD), a promising inerter-based device for vibration control of civil structures, to make the most of mass amplification and damping enhancement effect for the first time. As is common for tuned-type control devices, the TVMD control performance is significantly influenced by its design parameters. Following the well-known fixed-point theory [38,39], Ikago and Saito [36] proposed a closed-form solution to determine the TVMD design parameters. Huang and Hua [40] investigated the optimal design of the TVMD with linear and nonlinear viscous damping properties and found that a nonlinear TVMD can achieve comparable or even slightly better control

* Corresponding author.
E-mail address: HHe@hnit.edu.cn (H. He).

https://doi.org/10.1016/j.istruc.2023.03.112
Received 11 January 2023; Received in revised form 18 March 2023; Accepted 20 March 2023
2352-0124/

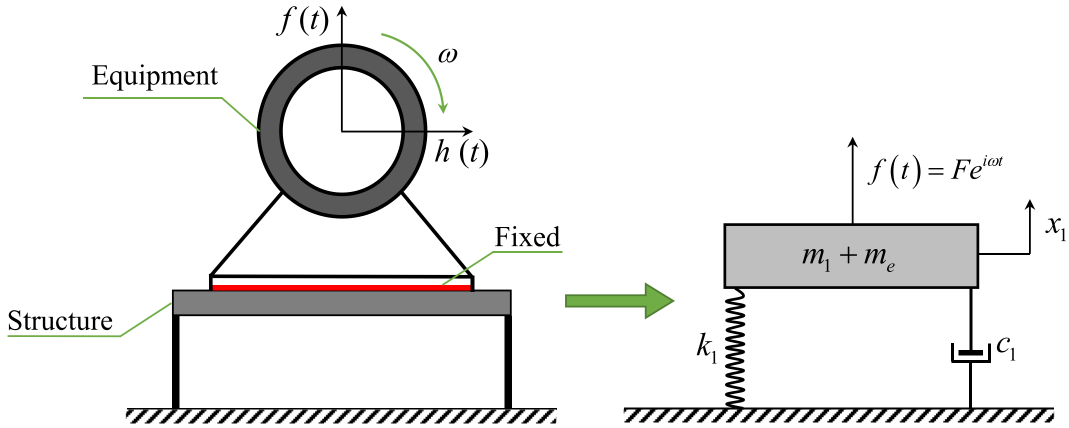

Fig. 1. Schematic of an SDOF main structure coupled with rotary mechanical equipment.

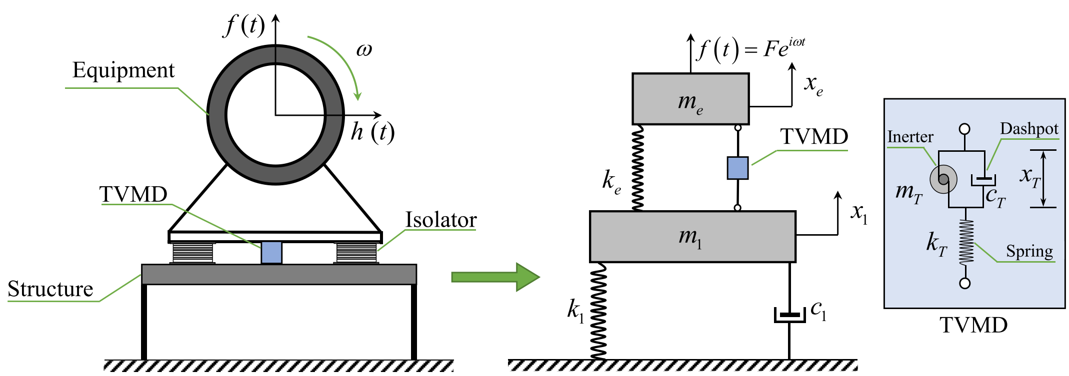

Fig. 2. Analytical model of TVMD isolation system.

performance than a linear TVMD. Considering the stochastic characteristics of seismic excitations, Pan and Zhang [41] developed a demand-based optimal design method for TVMDs to overcome some deficiencies of the fixed-point theory. To ensure that the control effectiveness of TVMDs becomes superior to that of the viscous damper with the same damping coefficient, He and Tan [42,43] proposed closed-form solutions of optimum design parameters of TVMDs based on the effective damping ratio enhancement effect. Concerning the nonstationary impulsive characteristics of seismic excitations, Su and Bian [44] developed an impulsive resistant optimization design method for TVMDs based on stability maximization. In addition, many excellent studies have been conducted on the development of inerter-based isolation systems for vibration mitigation of main structures subjected to seismic excitations [22–28,45]. The closest research to this study was carried out by Li and Chen [46], who focused on investigating the optimal design and performance evaluation of TVMD isolation systems under the white-noise seismic excitation hypothesis.

However, for industrial buildings, undesired vibration problems may be induced by rotary mechanical equipment (Fig. 1), which is distinguished from seismic excitation. Moreover, some industrial buildings have strict requirements for equipment vibration [47–50]. This suggests that the application of conventional isolation systems may not be appropriate considering their large displacements. Therefore, to provide an improved isolation control scheme, it is valuable to explore the application of TVMD isolation systems for equipment-induced vibration control of industrial buildings. In this study, considering that the external force is harmonic, a closed-form solution for optimum design parameters of TVMD isolation systems is proposed. This solution is theoretically based on the fixed-point theory. The design procedure of TVMD isolation systems is provided to balance the vibrations of the main structure and equipment. The validation of TVMD isolation systems is conducted based on a real industrial building. The numerical analysis results confirm that TVMD isolation systems can be used as an effective control strategy to solve the comfort problem of industrial buildings induced by rotary mechanical equipment.

2. Theoretical analysis

In this section, the undesired vibration problem induced by rotary mechanical equipment in industrial buildings is described. A classical analytical model for a single-degree-of-freedom (SDOF) main structure coupled with rotary mechanical equipment is provided. Moreover, an analytical model of TVMD isolation systems is established.

2.1. Structure coupled with rotary mechanical equipment

As is common in rotary mechanical equipment, centrifugal force occurs when the equipment operates with angular velocity ω, as shown in Fig. 1. Let $f(t)$ and $h(t)$ denote the vertical and horizontal components of centrifugal force, respectively. In this study, the stiffness of the main structure in the vertical direction is expected to be smaller than that in the horizontal direction. Furthermore, the main structure and equipment are more likely to resonate in the vertical direction, which may cause undesired comfort problems for the main structure and low working efficiency of the equipment. Therefore, only the vertical vibration caused by $f(t)$ is considered in this study.

Fig. 1 shows the main structure coupled with rotary mechanical equipment, where m_1, k_1, and c_1 are the mass, stiffness, and damping of the main structure, respectively; m_e is the mass of the equipment; and x_1 is the displacement of the main structure relative to the ground. Assuming that the vertical component of the centrifugal force is harmonic (i.e., $f(T) = Fe^{i\omega T}$), the governing equations of the system motion

Table 1
Notation.

	Notation	Definition
Main structure	m_1	Mass
	k_1	Stiffness coefficient
	c_1	Damping coefficient
	$\omega_1 = \sqrt{k_1/m_1}$	Frequency
	$\xi_1 = c_1/(2m_1\omega_1)$	Damping ratio
Excitation	$f(T) = Fe^{i\omega T}$	Excitation force; vertical component of the centrifugal force
	ω	Angular velocity of equipment; excitation frequency
	$\lambda = \omega/\omega_1$	Excitation frequency ratio
TVMD isolation system	m_e	Mass of the equipment
	k_e	Vertical equivalent stiffness coefficient of the isolator
	$\omega_e = \sqrt{k_e/m_e}$	Frequency of the isolator
	$\mu = m_e/m_1$	Equipment mass ratio
	$\alpha = \omega_e/\omega_1$	Frequency ratio of the isolator
	m_T	TVMD inertance
	k_T	TVMD stiffness coefficient
	c_T	TVMD damping coefficient
	$\omega_T = \sqrt{k_T/m_T}$	TVMD frequency
	$\xi_T = c_T/(2m_1\omega_1)$	TVMD damping ratio
	$\beta = m_T/m_1$	TVMD mass ratio
	$\gamma = \omega_T/\omega_1$	TVMD frequency ratio
Acceleration dynamic amplification factor (DAF)	$H_{1,0}$	Noncontrolled main structure and equipment
	$H_{1,\text{ TVMD}}$	Main structure controlled by the TVMD isolation system
	$H_{e,\text{ TVMD}}$	Equipment controlled by the TVMD isolation system
Response mitigation ratio (RMR)	$J_1 = \dfrac{\lvert H_{1,\text{ TVMD}}\rvert_{\max}}{\lvert H_{1,0}\rvert_{\max}}$	Main structure
	$J_e = \dfrac{\lvert H_{e,\text{ TVMD}}\rvert_{\max}}{\lvert H_{1,0}\rvert_{\max}}$	Equipment

can be written as

$$(m_1 + m_e)\ddot{x}_1 + c_1\dot{x}_1 + k_1x_1 = Fe^{i\omega t}. \tag{1}$$

The equipment is assumed to be fixed on the main structure, as shown in Fig. 1, and the acceleration dynamic amplification factor (DAF) for the noncontrolled main structure and equipment is obtained via the Fourier transform as follows [6]:

$$H_{1,0}(\lambda) = \frac{m_1U_1}{F} = \frac{\lambda^2}{\sqrt{\left[1-(1+\mu)\lambda^2\right]^2 + (2\zeta_1\lambda)^2}}, \tag{2}$$

where U_1 is the acceleration amplitude of the main structure; $\lambda = \omega/\omega_1$ is the excitation frequency ratio; ω_1 is the frequency of the main structure; ξ_1 is the damping ratio of the main structure; and μ denotes the equipment mass ratio. Note that although in this study we only investigated vertical vibration, relevant methods can still be employed for horizontal vibration control of the system by substituting the horizontal parameters for vertical ones (e.g., replacing $f(t)$ with $h(t)$).

2.2. Analytical model of TVMD isolation system

In this study, the improved performance of an isolation system provided by a TVMD is investigated. The isolation system coupled with the TVMD jointly constitutes the TVMD isolation system, as illustrated in Fig. 2. Herein, the vertical vibration damping of the equipment is expected to be provided by the TVMD, because the vertical equivalent damping of the isolator is assumed to be very small and can be ignored. Assuming that k_e denotes the vertical equivalent stiffness of the isolator; m_T, k_T, and c_T represent the TVMD inertance, stiffness, and damping coefficient, respectively; and x_T denotes the deformation of the TVMD inerter element. The TVMD isolation system governing equations of motion can be obtained as follows:

$$\begin{bmatrix} m_1 & 0 & 0 \\ 0 & m_e & 0 \\ 0 & 0 & m_T \end{bmatrix}\begin{Bmatrix} \ddot{x}_1 \\ \ddot{x}_e \\ \ddot{x}_T \end{Bmatrix} + \begin{bmatrix} c_1 & 0 & 0 \\ 0 & 0 & 0 \\ 0 & 0 & c_T \end{bmatrix}\begin{Bmatrix} \dot{x}_1 \\ \dot{x}_e \\ \dot{x}_T \end{Bmatrix} + \begin{bmatrix} k_1+k_e+k_T & -k_e-k_T & k_T \\ -k_e-k_T & k_e+k_T & -k_T \\ k_T & -k_T & k_T \end{bmatrix}\begin{Bmatrix} x_1 \\ x_e \\ x_T \end{Bmatrix} = \begin{Bmatrix} 0 \\ F \\ 0 \end{Bmatrix}e^{i\omega t}. \tag{3}$$

By introducing the TVMD mass ratio $\beta = m_T/m_1$, frequency ratio $\gamma = \omega_T/\omega_1$, damping ratio $\xi_T = c_T/(2m_1\omega_1)$, and isolator frequency ratio $\alpha = \omega_e/\omega_1$, as presented in Table 1, Eq. (3) can be rewritten as

$$\begin{bmatrix} 1 & 0 & 0 \\ 0 & \mu & 0 \\ 0 & 0 & \beta \end{bmatrix}\begin{Bmatrix} \ddot{x}_1 \\ \ddot{x}_e \\ \ddot{x}_T \end{Bmatrix} + \begin{bmatrix} 2\zeta_1\omega_1 & 0 & 0 \\ 0 & 0 & 0 \\ 0 & 0 & 2\zeta_T\omega_1 \end{bmatrix}\begin{Bmatrix} \dot{x}_1 \\ \dot{x}_e \\ \dot{x}_T \end{Bmatrix}$$
$$+ \begin{bmatrix} (1+\mu\alpha^2+\beta\gamma^2)\omega_1^2 & -(\mu\alpha^2+\beta\gamma^2)\omega_1^2 & \beta\gamma^2\omega_1^2 \\ -(\mu\alpha^2+\beta\gamma^2)\omega_1^2 & (\mu\alpha^2+\beta\gamma^2)\omega_1^2 & -\beta\gamma^2\omega_1^2 \\ \beta\gamma^2\omega_1^2 & -\beta\gamma^2\omega_1^2 & \beta\gamma^2\omega_1^2 \end{bmatrix}\begin{Bmatrix} x_1 \\ x_e \\ x_T \end{Bmatrix} = \begin{Bmatrix} 0 \\ F/m_1 \\ 0 \end{Bmatrix}e^{i\omega t}. \tag{4}$$

Similarly, let U_e denote the acceleration amplitude of the equipment, the acceleration DAF for the main structure and equipment controlled by the TVMD isolation system can be respectively expressed as.

$$H_{1,\text{TVMD}}(\lambda) = \frac{m_1U_1}{F} = \sqrt{\frac{A_1^2+B_1^2}{D^2+E^2}} \text{and} H_{e,\text{TVMD}}(\lambda) = \frac{m_1U_e}{F} = \sqrt{\frac{A_e^2+B_e^2}{D^2+E^2}}, \tag{5}$$

where

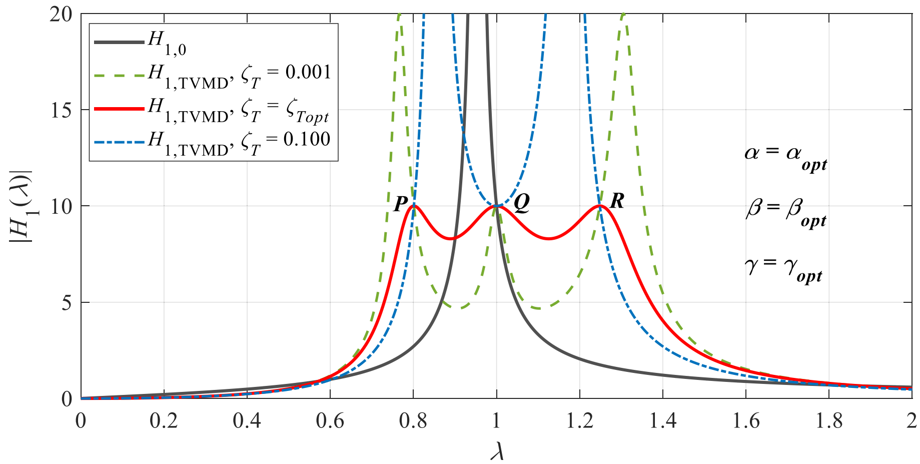

Fig. 3. Acceleration DAF of the undamped main structure for different values of ξ_T and $\mu = 0.1$.

$$\left\{\begin{array}{c} A_1 = -\mu\alpha^2\beta\gamma^2\lambda^2 + \left(\mu\alpha^2\beta + \beta^2\gamma^2\right)\lambda^4 \\ B_1 = -2\zeta_T\left(\mu\alpha^2 + \beta\gamma^2\right)\lambda^3 \\ A_e = -\beta\gamma^2\left(1 + \mu\alpha^2\right)\lambda^2 + \left[\beta\left(1 + \mu\alpha^2 + \beta\gamma^2 + \gamma^2\right) + 4\zeta_1\zeta_T\right]\lambda^4 - \beta\lambda^6 \\ B_e = 2(\zeta_T + \beta\zeta_1)\lambda^5 - 2\left[\zeta_T\left(1 + \beta\gamma^2 + \mu\alpha^2\right) + \beta\gamma^2\zeta_1\right]\lambda^3 \\ D = \mu\alpha^2\beta\gamma^2 - \left[\beta\gamma^2\left(\beta + \mu + \mu^2\alpha^2 + 4\zeta_1\zeta_T + \mu\alpha^2\right) + \mu\alpha^2(\beta + 4\zeta_1\zeta_T)\right]\lambda^2 \\ + \left[\mu\beta\left(1 + \gamma^2\right) + \left(\beta^2\gamma^2 + \mu\alpha^2\beta\right)(1 + \mu) + 4\mu\zeta_1\zeta_T\right]\lambda^4 - \mu\beta\lambda^6 \\ E = \left[2\beta\gamma^2\zeta_T + 2\mu\alpha^2\left(\zeta_T + \beta\gamma^2\zeta_1\right)\right]\lambda + 2\mu(\zeta_T + \beta\zeta_1)\lambda^5 \\ -\left[2\mu\zeta_T\left(\mu\alpha^2 + \alpha^2 + \beta\gamma^2 + 1\right) + 2\mu\zeta_1\left(\alpha^2\beta + \beta\gamma^2\right) + 2\beta\gamma^2\left(\mu\zeta_1 + \zeta_T\right)\right]\lambda^3 \end{array}\right. . \tag{6}$$

3. Optimal design of TVMD isolation system

In this section, a closed-form solution for optimum design parameters of TVMD isolation systems is proposed. It is theoretically based on the fixed-point theory. Detailed parametric studies are carried out to verify the correctness of the proposed closed-form solution and investigate the crucial connection between the parameters of TVMD isolation systems and control effectiveness. Furthermore, the design procedure is summarized to provide a viable method for balancing the vibrations of the main structure and equipment.

3.1. Closed-form solution for optimum parameters

Assuming that the damping of the main structure can be ignored (i.e., $\xi_1 = 0$), the acceleration DAF for the main structure can be simplified as

$$H_{1,\mathrm{TVMD}}(\lambda) = \sqrt{\frac{\widetilde{A}_1^2 + \widetilde{B}_1^2\zeta_T^2}{\widetilde{D}^2 + \widetilde{E}^2\zeta_T^2}}, \tag{7}$$

where

$$\left\{\begin{array}{c} \widetilde{A}_1 = -\mu\alpha^2\beta\gamma^2\lambda^2 + \left(\mu\alpha^2\beta + \beta^2\gamma^2\right)\lambda^4 \\ \widetilde{B}_1 = -2\left(\mu\alpha^2 + \beta\gamma^2\right)\lambda^3 \\ \widetilde{D} = \mu\alpha^2\beta\gamma^2 - \left[\beta\gamma^2\left(\beta + \mu + \mu^2\alpha^2 + \mu\alpha^2\right) + \mu\alpha^2\beta\right]\lambda^2 \\ + \left[\mu\beta\left(1 + \gamma^2\right) + \left(\beta^2\gamma^2 + \mu\alpha^2\beta\right)(1 + \mu)\right]\lambda^4 - \mu\beta\lambda^6 \\ \widetilde{E} = \left[2\beta\gamma^2 + 2\mu\alpha^2\right]\lambda + 2\mu\lambda^5 - \left[2\mu\left(\mu\alpha^2 + \alpha^2 + \beta\gamma^2 + 1\right) + 2\beta\gamma^2\right]\lambda^3 \end{array}\right. . \tag{8}$$

According to the fixed-point theory, the invariant points of $H_{1,\mathrm{TVMD}}(\lambda)$ are independent of ξ_T but are a function of λ. Therefore, it can substitute $\xi_T = 0$ and $\xi_T = \infty$ into Eqs. (7) and (8) to obtain

$$\frac{\widetilde{A}_1}{\widetilde{D}} = -\frac{\widetilde{B}_1}{\widetilde{E}}. \tag{9}$$

Thus,

$$a_3\left(\lambda^2\right)^3 + a_2\left(\lambda^2\right)^2 + a_1\lambda^2 + a_0 = 0, \tag{10}$$

where

$$\left\{\begin{array}{c} a_3 = 4\mu^2\alpha^2\beta + 4\mu\beta^2\gamma^2 \\ a_2 = -2\beta\left[\begin{array}{c} 2\mu^2(\mu+1)\alpha^4 + 2\mu^2\left(1 + \gamma^2 + 2\beta\gamma^2\right)\alpha^2 \\ + 4\mu\beta\gamma^2\alpha^2 + 2\beta^2\gamma^4(\mu+1) + \mu\beta\gamma^2\left(2 + \gamma^2\right) \end{array}\right] \\ a_1 = 2\beta\left[2\mu^2\left(1 + \gamma^2 + \mu\gamma^2\right)\alpha^4 + 2\mu\beta\gamma^4(\mu+1)\alpha^2 + \left(2\mu\gamma^2\alpha^2 + \beta\gamma^4\right)(\mu + 2\beta)\right] \\ a_0 = -4\mu\alpha^2\left(\mu\beta\gamma^2\alpha^2 + \beta^2\gamma^4\right) \end{array}\right. . \tag{11}$$

This implies that $H_{1,\mathrm{TVMD}}(\lambda)$ has three invariant points corresponding to the three real roots (i.e., λ_P^2, λ_Q^2, and λ_R^2 presented in Fig. 3) of Eq. (10), which can be expressed as

$$\lambda_P^2 = -\frac{a_2}{3a_3} + \sqrt[3]{-\frac{\Delta_1}{2} + \sqrt{\frac{\Delta_1^2}{4} + \frac{\Delta_2^3}{27}}} + \sqrt[3]{-\frac{\Delta_1}{2} - \sqrt{\frac{\Delta_1^2}{4} + \frac{\Delta_2^3}{27}}}, \tag{12a}$$

$$\lambda_Q^2 = -\frac{a_2}{3a_3} + \Delta_0\sqrt[3]{-\frac{\Delta_1}{2} + \sqrt{\frac{\Delta_1^2}{4} + \frac{\Delta_2^3}{27}}} + \Delta_0^2\sqrt[3]{-\frac{\Delta_1}{2} - \sqrt{\frac{\Delta_1^2}{4} + \frac{\Delta_2^3}{27}}}, \tag{12b}$$

$$\lambda_R^2 = -\frac{a_2}{3a_3} + \Delta_0^2\sqrt[3]{-\frac{\Delta_1}{2} + \sqrt{\frac{\Delta_1^2}{4} + \frac{\Delta_2^3}{27}}} + \Delta_0\sqrt[3]{-\frac{\Delta_1}{2} - \sqrt{\frac{\Delta_1^2}{4} + \frac{\Delta_2^3}{27}}}, \tag{12c}$$

where

$$\Delta_0 = \frac{-1 + \sqrt{-3}}{2}, \Delta_1 = \frac{27a_3^2a_0 - 9a_3a_2a_1 + 2a_2^3}{27a_3^3}, \Delta_2 = \frac{3a_3a_1 - a_2^2}{3a_3^2}. \tag{13}$$

The optimal condition yields[42]

$$\left|H_{1,\mathrm{TVMD}}(\lambda_P)\right| = \left|H_{1,\mathrm{TVMD}}(\lambda_Q)\right| = \left|H_{1,\mathrm{TVMD}}(\lambda_R)\right|. \tag{14}$$

By solving Eq. (14), the closed-form solution for optimum values of α, β, and γ can be expressed as

$$\alpha_{opt} = \sqrt{\frac{1}{2\mu + 1}}, \beta_{opt} = \frac{2\mu^2}{(2\mu + 1)^2}, \gamma_{opt} = \sqrt{2\mu + 1}. \tag{15}$$

Substituting Eq. (15) into Eq. (12) we obtain

$$\lambda_P^2 = 1 + \mu - \sqrt{\mu(2 + \mu)}, \lambda_Q^2 = 1, \lambda_R^2 = 1 + \mu + \sqrt{\mu(2 + \mu)}. \tag{16}$$

To ensure that $H_{1,\mathrm{TVMD}}(\lambda)$ achieves the maximum value at the three invariant points, the damping ratio of the TVMD isolation system should yield.

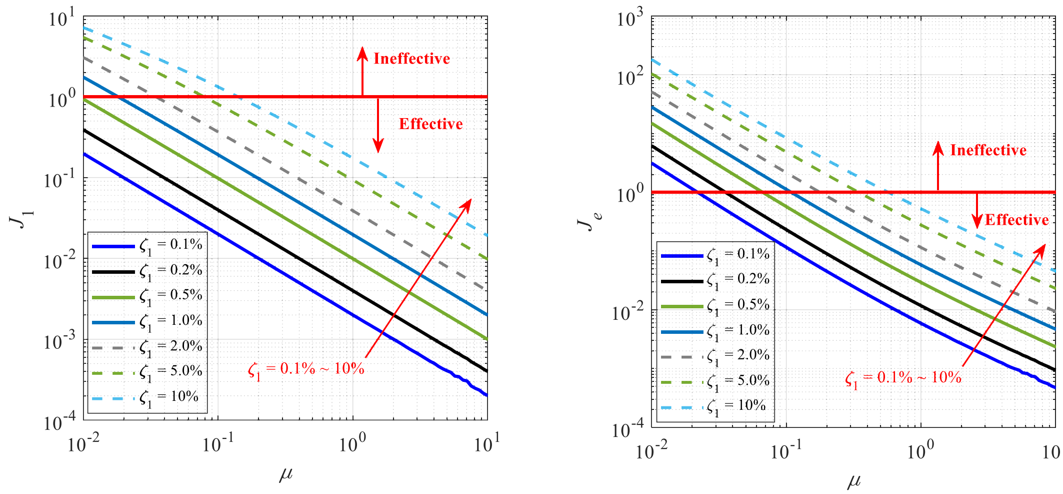

(a) Structure (b) Equipment

Fig. 4. Analysis results of RMR for the damped main structure and equipment when $0.01 \leqslant \mu \leqslant 10$ and $0.1\% \leqslant \xi_1 \leqslant 10\%$. (a) Structure and (b) equipment.

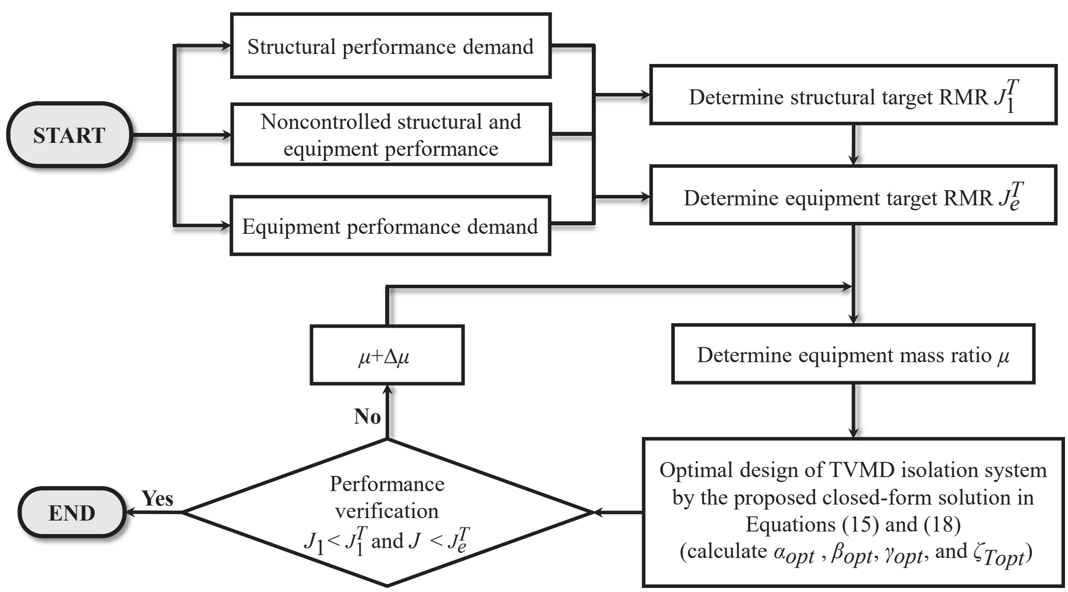

Fig. 5. Flowchart of the TVMD isolation system design procedure.

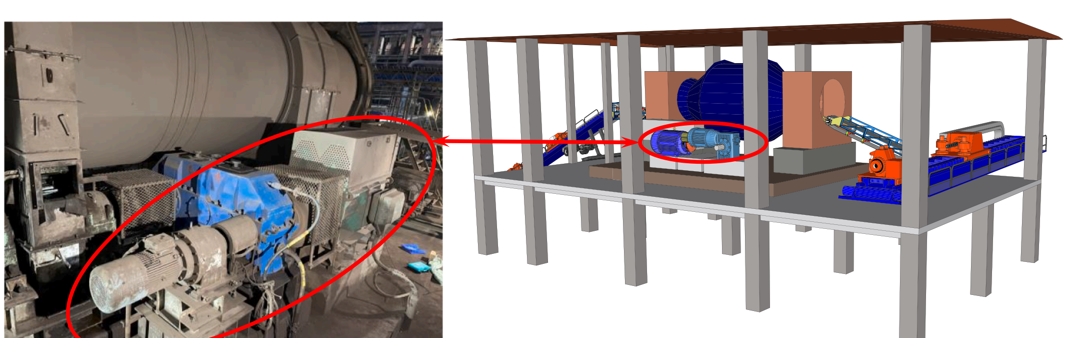

Fig. 6. Illustration of the numerical model.

Table 2
Model parameters.

Main structure		Excitation force $f(T) = Fe^{i\omega T}$	
Mass m_1 (ton)	90.30	Amplitude F (kN)	14.90
Frequency ω_1 (Hz)	16.67	Frequency ω (Hz)	16.41
Damping ratio ξ_1	0.20%	Frequency ratio λ	0.98

$$\left.\frac{\partial\{|H_{1,\mathrm{TVMD}}(\lambda)|\}^2}{\partial\lambda^2}\right|_{\lambda^2=\lambda_P^2}, \left.\frac{\partial\{|H_{1,\mathrm{TVMD}}(\lambda)|\}^2}{\partial\lambda^2}\right|_{\lambda^2=\lambda_Q^2}, \text{and} \left.\frac{\partial\{|H_{1,\mathrm{TVMD}}(\lambda)|\}^2}{\partial\lambda^2}\right|_{\lambda^2=\lambda_R^2}. \tag{17}$$

Combining Equations (16) and (17), the closed-form solution for optimum ξ_T can be expressed as

$$\zeta_{Topt} = \frac{\sqrt{2\mu^5}}{4\mu^2+4\mu+1}. \tag{18}$$

According to the optimum parameters of the TVMD isolation system, and substituting Eqs. (15) and (18) into Eq. (7), the maximum value of $H_{1,\ \mathrm{TVMD}}(\lambda)$ at the three invariant points is expressed as

$$|H_{1,\mathrm{TVMD}}|_{\max} = \frac{1}{\mu}. \tag{19}$$

Clearly, the control effectiveness of the TVMD isolation system for the undamped main structure is negatively related to the equipment mass ratio μ, that is, the TVMD isolation system becomes more effective as μ increases.

3.2. Parametric study

It is known that all acceleration DAF $H_{1,\ \mathrm{TVMD}}(\lambda)$ curves of the undamped main structure for different values of the damping ratio ξ_T will pass the three invariant points (i.e., P, Q, and R), which are also the peaks of $H_{1,\ \mathrm{TVMD}}(\lambda)$ if the TVMD isolation system is optimally designed using the fixed-point theory. Considering that the equipment mass ratio μ is 0.1, $H_{1,\ \mathrm{TVMD}}(\lambda)$ of the undamped main structure for different values of ξ_T can be obtained, as shown in Fig. 3. Note that $H_{1,\ \mathrm{TVMD}}(\lambda)$ achieves its maximum value at the three invariant points. This means that the closed-form solution for optimum parameters of TVMD isolation systems proposed in Section 3.1 satisfies the requirements of the fixed-point theory, which demonstrates the correctness of the proposed solution. Compared to the acceleration DAF $H_{1,0}(\lambda)$ for a noncontrolled main structure, the maximum value of $H_{1,\ \mathrm{TVMD}}(\lambda)$ is extremely suppressed near the resonance region when the TVMD isolation system is optimally designed. Notably, the TVMD isolation system is expected to control the response of the main structures near the resonance region. Beyond the resonance region, the TVMD isolation system shows weak or negative control effectiveness. Therefore, the reduction in the maximum value of the acceleration DAF is considered more appropriate as a performance index to evaluate the control effectiveness of the TVMD isolation system.

Note that the maximum value of the acceleration DAF for the main structure should be minimized when the TVMD isolation system is optimally designed using the fixed-point theory. To demonstrate the control effectiveness of the optimally designed TVMD isolation system, the response mitigation ratio (RMR) can be defined as.

$$J_1 = \frac{|H_{1,\mathrm{TVMD}}|_{\max}}{|H_{1,0}|_{\max}} \text{ and } J_e = \frac{|H_{e,\mathrm{TVMD}}|_{\max}}{|H_{1,0}|_{\max}}, \tag{20}$$

Table 3
Design results of TVMD and conventional isolation systems.

Parameters	TVMD isolation systems			Conventional isolation systems		
	Case 1	Case 2	Case 3	Case 1a	Case 2a	Case 3a
m_e(ton)	3.07	9.03	27.09	3.07	9.03	27.09
μ	0.034	0.100	0.300	0.034	0.100	0.300
α	0.9676	0.9129	0.7906	0.9676	0.9129	0.7906
β	0.0020	0.0139	0.0703	–	–	–
γ	1.0334	1.0954	1.2649	–	–	–
ξ_T	2.64×10^{-4}	3.11×10^{-3}	2.72×10^{-2}	2.64×10^{-4}	3.11×10^{-3}	2.72×10^{-2}
k_e(kN/m)	3.15×10^4	8.26×10^4	1.86×10^5	3.15×10^4	8.26×10^4	1.86×10^5
m_T(kg)	183.03	1254.17	6349.22	–	–	–
k_T(kN/m)	2.14×10^3	1.65×10^4	1.11×10^5	–	–	–
c_T or c_e (kN·s/m)	4.50	58.75	512.12	4.50	58.75	512.12

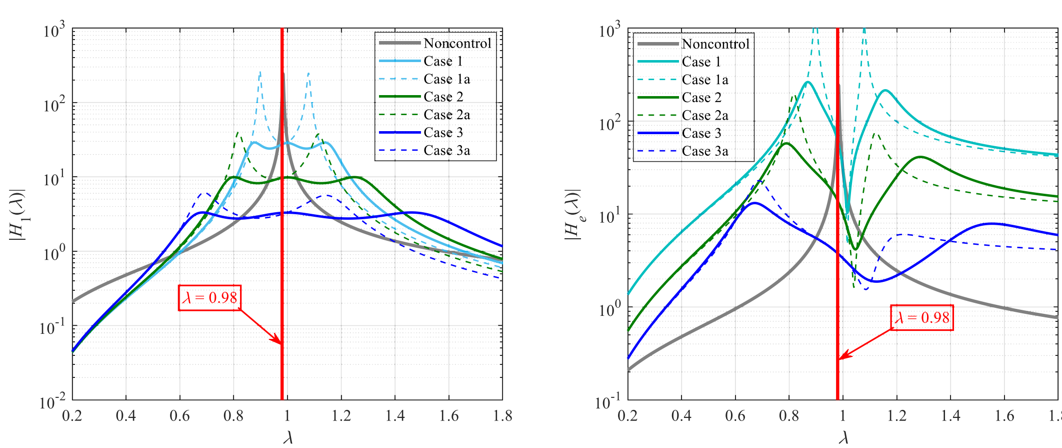

(a) Structure (b) Equipment

Fig. 7. Comparison results of acceleration DAF for the main structure and equipment. (a) Structure and (b) equipment.

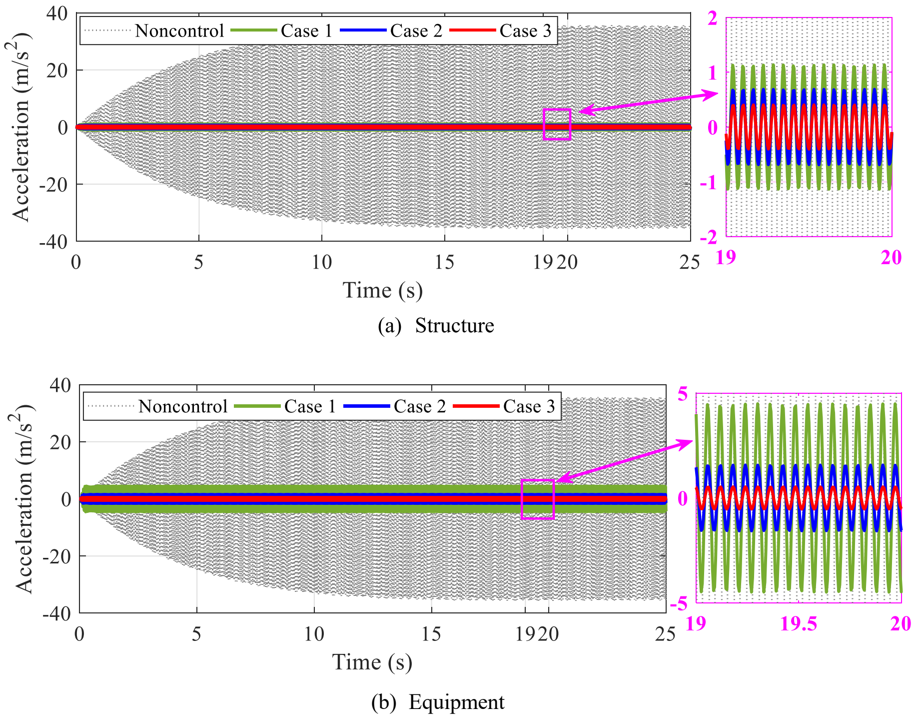

Fig. 8. Time-history analysis results of acceleration responses of the main structure and equipment. (a) Structure and (b) equipment.

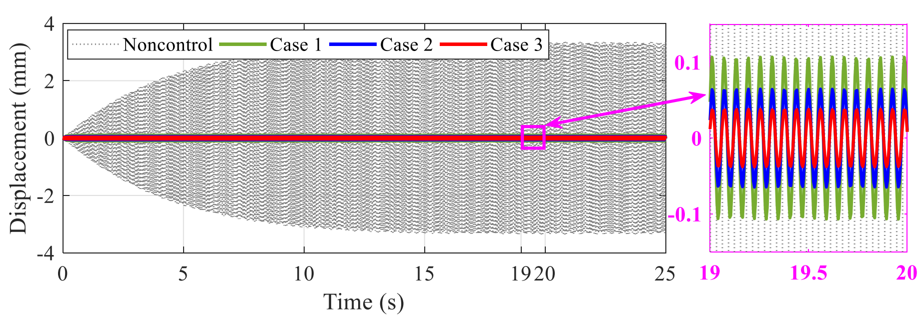

Fig. 9. Time-history analysis results of displacement responses of the main structure.

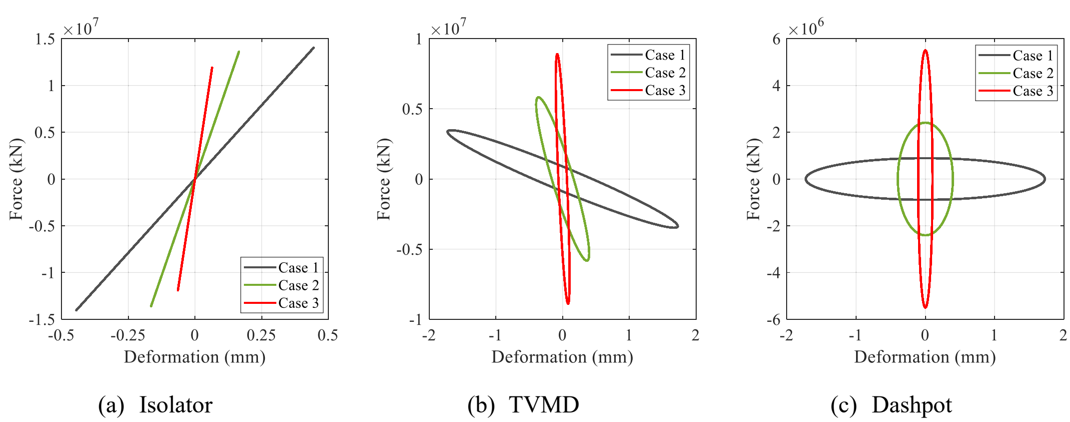

Fig. 10. The hysteretic curve of TVMD isolation systems. (a) Isolator, (b) TVMD, and (c) dashpot.

where J_1 and J_e denote the RMR for the main structure and equipment controlled by the TVMD isolation system, respectively. Clearly, the TVMD isolation system shows positive control effectiveness for the main structure and equipment only if J_1 and J_e are less than one.

As shown in Fig. 4, J_1 and J_e are positively related to μ, that is, increasing the equipment mass can improve the effectiveness of the TVMD isolation system in terms of the acceleration response of both the main structure and equipment. Furthermore, J_1 and J_e are negatively related to the structural damping ratio ξ_1. This implies that increasing the damping ratio of the main structure weakens the control

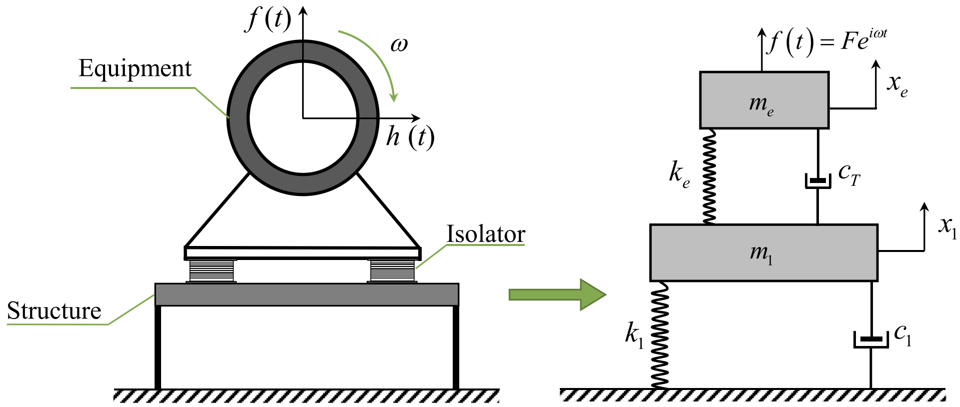

Fig. A1. Analytical model for the conventional isolation system.

effectiveness of the TVMD isolation system. In the case of a low-damping main structure (e.g., $\xi_1 \leqslant 1.0\%$), the TVMD isolation system shows positive control effectiveness for both the main structure and equipment when $\mu \geqslant 0.1$. Additionally, the required value of μ increases to maintain this situation with an increment of ξ_1. Therefore, it is possible to balance the control effectiveness of the TVMD isolation system for the acceleration response of the main structure and equipment by adjusting the equipment mass ratio μ.

3.3. Design procedure

As presented in Fig. 5, the design procedure of TVMD isolation systems is provided to balance the vibrations of the main structure and equipment. According to the performance demand (e.g., the specified restriction of maximum acceleration response), the target RMR for the main structure and equipment can be determined as J_1^T and J_e^T, respectively. A TVMD isolation system can be optimally designed using the proposed closed-form solution provided that the equipment mass ratio μ is predetermined in advance. If the TVMD isolation system fails the performance verification, as discussed in Section 3.2, a supplemental mass (corresponding to the mass ratio $\Delta\mu$) should be added to the equipment to enhance the control effectiveness. Following the above procedure, the key point of the design of TVMD isolation systems is to ensure that the vibrations of both the main structure and equipment satisfy the restrictions.

4. Application and validation of TVMD isolation system

In the previous sections, TVMD isolation systems were investigated via theoretical analysis. In this section, the application and validation of a TVMD isolation system based on a real industrial building are described. As illustrated in Fig. 6, an industrial building is prepared as a barrel mixer building for an ironmaking plant. Based on a preliminary survey, it is concluded that the comfort problem of the floor for this industrial building is induced by rotary mechanical equipment whose excitation frequency is in the resonance region. Therefore, the TVMD isolation system is supposed to be effective in controlling the vibrations of both the main structure and equipment. Herein, resonance modal parameters of the main structure are set as listed in Table 2.

To obtain different performance levels, Table 3 lists three TVMD isolation systems designed using the proposed closed-form solution, in which the equipment mass ratio μ is presented in ascending order (corresponding Cases 1, 2, and 3). To demonstrate the superior control performance of TVMD isolation systems over that of conventional isolation systems, three conventional isolation systems (corresponding Cases 1a, 2a, and 3a) are prepared in Table 3. The analytical model for the conventional isolation system is provided in Appendix A.

Fig. 7 shows comparison results of acceleration DAF for the main structure and equipment. It is confirmed that TVMD isolation systems are effective in controlling the maximum response of both the main structure and equipment near the resonance region. The effective region becomes larger for TVMD isolation systems with increasing equipment mass ratio μ. Three peaks of acceleration DAF for the main structure are very close (the difference is within 1%) in different cases, indicating that the proposed closed-form solution can still provide a good estimate for optimum design parameters of TVMD isolation systems even if the fixed-point theory no longer holds for the damped main structure (i.e., $\xi_1 \neq 0$). It is observed that TVMD isolation systems are more effective in controlling the maximum response of both the main structure and equipment compared to conventional isolation systems. However, TVMD isolation systems are not always better than conventional isolation systems throughout the frequency domain. For example, conventional isolation systems have a slightly better control performance for the main structure than TVMD isolation systems when $\lambda = 0.98$ in the case of equipment mass ratios are 0.100 and 0.300. Therefore, the application of tuned viscous mass damper isolation systems for equipment-induced vibration control of industrial buildings is particularly recommended under the evaluation system of the fixed-point theory where the maximum value of acceleration DAF for the main structure and equipment is the primary control objective.

To further investigate the control effectiveness of the TVMD isolation system, a time-history analysis is conducted according to the parameters listed in Tables 2 and 3. Fig. 8 shows the results of this time-history analysis in terms of the acceleration responses of the main structure and equipment. It is observed that the maximum acceleration response of the noncontrolled main structure is 35.66 m/s^2, which is suppressed by 96.81%, 98.07%, and 98.86% for Cases 1, 2, and 3, respectively. The TVMD shows vibration mitigation ratios of 87.30 %, 95.57 %, and 98.50% for the maximum acceleration response of the equipment. The control effectiveness of TVMD isolation systems for the main structure is slightly better than that of equipment. This is because the closed-form solution for optimum design parameters of TVMD isolation systems is proposed based on the acceleration DAF of the main structure. It can be concluded that TVMD isolation systems optimally designed using the proposed closed-form solution are highly effective in controlling the acceleration response of both the main structure and equipment. Thus, TVMD isolation systems can be considered as an effective control strategy to solve the comfort problem of industrial buildings induced by rotary mechanical equipment.

Fig. 9 presents the time-history analysis results of displacement responses of the main structure. It is seen that the maximum displacement response of the noncontrolled main structure is 3.35 mm, which is reduced by 96.81%, 98.07%, and 98.87% for Cases 1, 2, and 3, respectively. Concerning equipment, in combination with Fig. 10(a), the corresponding maximum displacement reductions are 87.91%, 95.13%, and 98.08% for Cases 1, 2, and 3, respectively. Therefore, TVMD isolation systems optimally designed using the proposed closed-form solution are also highly effective in controlling the displacement response of both the main structure and equipment. TVMD isolation systems become more effective with increasing equipment mass ratio μ, which coincides with Eq. (19). However, the displacement response is relatively small compared with the acceleration response, which rarely causes safety problems in industrial buildings. Thus, the comfort problem induced by the acceleration response is the primary control objective of the TVMD isolation system in this study.

As observed in Fig. 10, the deformation of the TVMD is amplified by factors of 3.87, 2.39, and 1.59 for Cases 1, 2, and 3, respectively, compared to that of the isolator. This reveals that the deformation of the inner degree of freedom in the TVMD is amplified when the TVMD is tuned to resonate with the main structure (i.e., frequency ratio γ close to 1.0), which can be referred to as the damping enhancement (DE) effect [51]. As γ increases away from 1.0 as listed in Table 3, the DE effect of the TVMD becomes less remarkable. Therefore, the equipment mass ratio μ as well as the corresponding frequency ratio γ can be adjusted in practical applications to ensure that TVMD isolation systems have an improved energy dissipation ability.

From the above analysis results, it can be concluded that TVMD isolation systems optimally designed using the proposed closed-form solution are effective in controlling the acceleration and displacement responses of both the main structure and equipment. TVMD isolation systems can be considered as an effective control strategy to solve the comfort problem of industrial buildings induced by rotary mechanical equipment. This is because the inner degree of freedom in a TVMD is amplified when the TVMD is tuned to resonate with the main structure, which provides a significantly improved energy-dissipation ability of the TVMD isolation system.

5. Conclusions

In this study, the application of TVMD isolation systems for equipment-induced vibration control in industrial buildings is investigated. A closed-form solution for optimum design parameters of TVMD isolation systems is proposed. Validation of a TVMD isolation system is conducted on a real industrial building. The main conclusions of this study can be summarized as follows:

1) A closed-form solution for optimum design parameters of TVMD isolation systems based on the fixed-point theory is proposed. For a damped main structure, the proposed closed-form solution can still provide a good estimate for optimum design parameters of TVMD isolation systems, even if the fixed-point theory no longer holds.
2) TVMD isolation systems are expected to control the response of the main structures near the resonance region. Beyond this region, TVMD isolation systems show weak or negative control effectiveness.
3) The design procedure of TVMD isolation systems is provided to balance the vibrations of the main structure and equipment. Optimally designed TVMD isolation systems are effective in controlling the acceleration and displacement responses of both the main structure and equipment.
4) TVMD isolation systems can be considered as an effective control strategy to solve the comfort problem of industrial buildings induced by rotary mechanical equipment. This is because the inner degree of freedom in TVMD is amplified when the TVMD is tuned to resonate with the main structure, which provides a significantly improved energy-dissipation ability of the TVMD isolation system.

In this study, the closed-form solution for optimum design parameters of TVMD isolation systems is proposed based on the acceleration DAF for the main structure. In the future, the closed-form solution for optimum design parameters of TVMD isolation systems should be investigated based on the acceleration DAF of the equipment if the precision and function of the equipment are major concerns.

Declaration of Competing Interest

The authors declare that they have no known competing financial interests or personal relationships that could have appeared to influence the work reported in this paper.

Acknowledgments

This study is supported by the National Natural Science Foundation of China (No. 51878264; 52278306); the Key Research and Development Program of Hunan Province, China (No. 2022SK2096); the Science and Technology Progress and Innovation Project of the Department of Transportation of Hunan Province, China (No. 201912); the Scientific Research Project of Hunan Education Department, China (No. 22B0858); the Science and Technology Innovation Project of Hengyang City, China (No. 202250045150); and the Introduction of Talent Research Project of Hunan Institute of Technology, China (No. HQ22019).

Appendix A. Analytical model for conventional isolation system

Fig. A1 shows the analytical model for the conventional isolation system installed between the main structure and equipment. Herein, the vertical vibration damping of the equipment is expected to be provided by the isolator. Assuming that c_T is the vertical equivalent damping of the isolator, the conventional isolation system governing equations of motion can be obtained as:

$$\begin{bmatrix} m_1 & 0 \\ 0 & m_e \end{bmatrix}\begin{Bmatrix} \ddot{x}_1 \\ \ddot{x}_e \end{Bmatrix} + \begin{bmatrix} c_1 + c_T & -c_T \\ -c_T & c_T \end{bmatrix}\begin{Bmatrix} \dot{x}_1 \\ \dot{x}_e \end{Bmatrix} + \begin{bmatrix} k_1 + k_e & -k_e \\ -k_e & k_e \end{bmatrix}\begin{Bmatrix} x_1 \\ x_e \end{Bmatrix} = \begin{Bmatrix} 0 \\ F \end{Bmatrix} e^{i\omega t} \tag{A1}$$

Note that the damping of the isolator is assumed to be equal to that of TVMD for a fair performance comparison between TVMD and conventional isolation systems. For non-dimensional analysis, Eq. (A1) can be rewritten as

$$\begin{bmatrix} 1 & 0 \\ 0 & \mu \end{bmatrix}\begin{Bmatrix} \ddot{x}_1 \\ \ddot{x}_e \end{Bmatrix} + \begin{bmatrix} 2(\zeta_1 + \zeta_T)\omega_1 & -2\zeta_T\omega_1 \\ -2\zeta_T\omega_1 & 2\zeta_T\omega_1 \end{bmatrix}\begin{Bmatrix} \dot{x}_1 \\ \dot{x}_e \end{Bmatrix} + \begin{bmatrix} (1+\mu\alpha^2)\omega_1^2 & -\mu\alpha^2\omega_1^2 \\ -\mu\alpha^2\omega_1^2 & \mu\alpha^2\omega_1^2 \end{bmatrix}\begin{Bmatrix} x_1 \\ x_e \end{Bmatrix} = \begin{Bmatrix} 0 \\ \dfrac{F}{m_1} \end{Bmatrix} e^{i\omega t}. \tag{A2}$$

Further, the acceleration DAF for the main structure and equipment controlled by the conventional isolation system can be respectively given as.

$$H_{1,\mathrm{CI}} = \sqrt{\frac{(\mu\alpha^2\lambda^2)^2 + (2\zeta_T\lambda^3)^2}{\Omega}} \text{ and } H_{e,\mathrm{CI}} = \sqrt{\frac{\left[-(1+\mu\alpha^2)\lambda^2 + \lambda^4\right]^2 + \left[2(\zeta_1+\zeta_T)\lambda^3\right]^2}{\Omega}}, \tag{A3}$$

where the denominator Ω is

$$\Omega = \left[\mu\alpha^2 - \left(\mu^2\alpha^2 + \mu\alpha^2 + \mu + 4\zeta_1\zeta_T\right)\lambda^2 + \mu\lambda^4\right]^2 + \left[2\left(\mu\alpha^2\zeta_1 + \zeta_T\right)\lambda - 2\left(\zeta_T + \mu\zeta_T + \mu\zeta_1\right)\lambda^3\right]^2 \quad \text{(A4)}$$

The notations in the above equations are the same as those listed in Table 1.

References

[1] Yao JTP. Concept of structural control. J Struct Div 1972;98(7):1567–74.
[2] Housner GW, Bergman LA, Caughey TK, et al. Structural control: past, present, and future. J Eng Mech 1997;123(9):897–971.
[3] Spencer Jr BF, Nagarajaiah S. State of the art of structural control. J Struct Eng 2003;129(7):845–56.
[4] Soong TT, Spencer Jr BF. Supplemental energy dissipation: state-of-the-art and state-of-the-practice. Eng Struct 2002;24(3):243–59.
[5] Ma RS, Bi KM, Hao H. Inerter-based structural vibration control: a state-of-the-art review. Eng Struct 2021;243:112655.
[6] Guo XY, Zhu Y, Qu YG, Cao DX. Design and experiment of an adaptive dynamic vibration absorber with smart leaf springs. Appl Math Mech 2022;43(10):1485–502.
[7] Zhang WX, Zhang W, Yang DS, Luo Z, Guo XY. Vibration suppression of nonlinear laminated composite plates using internal oscillator-enhanced nonlinear energy sinks. Eng Struct 2023;279:115579.
[8] Hwang JS, Kim J, Kim YM. Rotational inertia dampers with toggle bracing for vibration control of a building structure. Eng Struct 2007;29(6):1201–8.
[9] Asai T, Watanabe Y. Outrigger tuned inertial mass electromagnetic transducers for high-rise buildings subject to long period earthquakes. Eng Struct 2017;153:404–10.
[10] Taflanidis AA, Giaralis A, Patsialis D. Multi-objective optimal design of inerter-based vibration absorbers for earthquake protection of multi-storey building structures. J Franklin Inst 2019;356(14):7754–84.
[11] Lu L, Xu JQ, Zhou Y, Lu WS, Spencer Jr BF. Viscous inertial mass damper (VIMD) for seismic responses control of the coupled adjacent buildings. Eng Struct 2021;233:111876.
[12] Hao LF, He H, Tan P. Response mitigation performance and energy dissipation enhancement of tuned viscous mass damper applied on adjacent structures. Soil Dyn Earthq Eng 2021;150:106902.
[13] Wang XR, He T, Shen YJ, Shan YC, Liu XD. Parameters optimization and performance evaluation for the novel inerter-based dynamic vibration absorbers with negative stiffness. J Sound Vib 2019;463:114941.
[14] Giaralis A, Taflanidis AA. Optimal tuned mass-damper-inerter (TMDI) design for seismically excited MDOF structures with model uncertainties based on reliability criteria. Struct Control Health Monit 2018;25(2):e2082.
[15] Shen WA, Niyitangamahoro A, Feng ZQ, Zhu HP. Tuned inerter dampers for civil structures subjected to earthquake ground motions: optimum design and seismic performance. Eng Struct 2019;198:109470.
[16] Xu K, Bi KM, Han Q, Li XP, Du XL. Using tuned mass damper inerter to mitigate vortex-induced vibration of long-span bridges: analytical study. Eng Struct 2019;182:101–11.
[17] Luo H, Zhang RF, Weng DG. Mitigation of liquid sloshing in storage tanks by using a hybrid control method. Soil Dyn Earthq Eng 2016;90:183–95.
[18] Zhang RF, Zhao ZP, Pan C. Influence of mechanical layout of inerter systems on seismic mitigation of storage tanks. Soil Dyn Earthq Eng 2018;114:639–49.
[19] Jiang YY, Zhao ZP, Zhang RF, De Domenico D, Pan C. Optimal design based on analytical solution for storage tank with inerter isolation system. Soil Dyn Earthq Eng 2020;129:105924.
[20] Hu Y, Wang J, Chen MZQ, Li Z, Sun Y. Load mitigation for a barge-type floating offshore wind turbine via inerter-based passive structural control. Eng Struct 2018;177:198–209.
[21] Ma RS, Bi KM, Hao H. Mitigation of heave response of semi-submersible platform (SSP) using tuned heave plate inerter (THPI). Eng Struct 2018;177:357–73.
[22] De Domenico D, Ricciardi G. Improving the dynamic performance of base-isolated structures via tuned mass damper and inerter devices: a comparative study. Struct Control Health Monit 2018;25(10):e2234.
[23] Etedali S, Hasankhoie K, Sohrabi MR. Seismic responses and energy dissipation of pure-friction and resilient-friction base-isolated structures: a parametric study. J Build Eng 2020;29:101194.
[24] Gao H, Xing CX, Wang H, Li J, Zhang Y. Performance improvement and demand-oriented optimum design of the tuned negative stiffness inerter damper for base-isolated structures. J Build Eng 2023;63:105488.
[25] Ariga T, Kanno Y, Takewaki I. Resonant behaviour of base-isolated high-rise buildings under long-period ground motions. Struct Design Tall Spec Build 2006;15:325–38.
[26] Li LY, Liang QG. Effect of inerter for seismic mitigation comparing with base isolation. Struct Control Health Monit 2019;26:e2409.
[27] Nyangi P, Ye K. Optimal design of dual isolated structure with supplemental tuned inerter damper based on performance requirements. Soil Dyn Earthq Eng 2021;149:106830.
[28] Tai YJ, Huang ZW, Chen C, Hua XG, Chen ZQ. Geometrically nonlinearity analysis and performance evaluation of tuned inerter dampers for multidirectional seismic isolation. Mech Syst Sig Process 2022;168:108681.
[29] Pan C, Zhang RF. Design of structure with inerter system based on stochastic response mitigation ratio. Struct Control Health Monit 2018;25(6):e2169.1–2169.21.
[30] Smith MC. Synthesis of mechanical networks: the inerter. IEEE Trans Autom Control 2002;47(10):1648–62.
[31] C. Papageorgiou M.C. Smith Laboratory experimental testing of inerters 2005 Spain 3351 3356.
[32] Force-Controlling SMC. Mechanical Device. Cambridge University technical services Ltd; 2008.
[33] Wang FC, Hong MF, Lin TC. Designing and testing a hydraulic inerter. *Proceedings of the Institution of Mechanical Engineers Part C Journal of Mechanical Engineering Science*. 2010, 225(1):66-72.
[34] Gonzalez-Buelga A, Clare LR, Neild SA, Jiang JZ, Inman DJ. An electromagnetic inerter-based vibration suppression device. Smart Mater Struct 2015;24(5):55015.
[35] Kawamata S. Development of a vibration control system of structures by means of mass pumps. Tokyo, Japan: Institute of Industrial Science, University of Tokyo; 1973.
[36] Ikago K, Saito K, Inoue N. Seismic control of single-degree-of-freedom structure using tuned viscous mass damper. Earthq Eng Struct Dyn 2012;41(3):453–74.
[37] Arai T, Aburakawa T, Ikago K, Hori N, Inoue N. Verification on effectiveness of a tuned viscous mass damper and its applicability to non-linear structural systems. J Struct Constr Eng 2009;645:1993–2002.
[38] Den Hartog JP. Mechanical vibration. NY: McGraw Hill; 1956.
[39] Ormondroyd J, Den Hartog JP. The theory of the dynamic vibration absorber. ASME J Appl Mech 1928;50:9–22.
[40] Huang ZW, Hua XG, Chen ZQ, Niu HW. Optimal design of TVMD with linear and nonlinear viscous damping for SDOF systems subjected to harmonic excitation. Struct Control Health Monit 2019;26:e2413.
[41] Pan C, Zhang RF, Luo H, Li C, Shen H. Demand-based optimal design of oscillator with parallel-layout viscous inerter damper. Struct Control Health Monit 2018;25:e2051.
[42] He H, Tan P, Hao LF, Xu K, Xiang Y. Optimal design of tuned viscous mass damper for acceleration response control of civil structures under seismic excitations. Eng Struct 2022;252:113685.
[43] He H, Tan P, Hao LF, Xu K, Xiang Y. Optimal design of tuned viscous mass dampers based on effective damping ratio enhancement effect. J Sound Vib 2022;534:117018.
[44] Su N, Bian J, Peng ST, Xia Y. Impulsive resistant optimization design of tuned viscous mass damper (TVMD) based on stability maximization. Int J Mech Sci 2023;239:107876.
[45] Liu CN, Chen L, Lee HP, Yang Y, Zhang XL. A review of the inerter and inerter-based vibration isolation: theory, devices, and applications. J Franklin Inst 2022;359(14):7677–707.
[46] Li YF, Li SY, Chen ZQ. Optimal design and effectiveness evaluation for inerter-based devices on mitigating seismic responses of base isolated structures. Earthq Eng Eng Vib 2021;20:1021–32.
[47] Liu XT, Wang W, Fang C. Seismic vibration control of novel prefabricated industrial equipment suspension structures with tuned mass damper. J Constr Steel Res 2022;191:107163.
[48] A. Tombari P. Cacciola I. Zentner Vibration control of an industrial building through the vibrating barrier 2015 Cambridge UK.
[49] A. Martelli State-of-the-art on the development and application of seismic vibration control techniques and some innovative strengthening methods for civil and industrial structures 2003 Prague.
[50] Tuhta S, Günday F. MIMO system identification of industrial building using N4SID with ambient vibration. Int J Innovat Eng Res Technol 2019.
[51] Zhang RF, Zhao ZP, Pan C, Ikago K, Xue ST. Damping enhancement principle of inerter system. Struct Control Health Monit 2020:e2523.